



## UNDERSTANDING THE FLOW AND SEDIMENT DYNAMICS IN THE MEKONG RIVER – A CASE STUDY IN THE VINH LONG PROVINCE

T.N.Q. Nga<sup>1</sup>, D.N. Khoi<sup>2</sup>, N.T.D. Thuy<sup>2</sup>, D.T. Nhan<sup>2</sup>, T.T. Kim<sup>3</sup> and N.T. Bay<sup>1</sup>

**ABSTRACT:** River bank processes of erosion and accretion are influenced by both of natural processes and human activities. Therefore, understanding the riverbank processes plays an important role in erosion and accretion mitigations in the Vietnamese Mekong Delta. The objective of this study is to investigate the response of flow and sediment dynamics under impacts of sand mining, river encroachment due to the expansion of fish ponds, and hydrological alteration from the upstream area – a case study in the Mekong River in the Vinh Long province by using MIKE 21 FM model. The calibration and validation results indicated that MIKE 21 FM is one of reliable and reasonable tools for simulating the flow and sediment dynamics in the study area. The responses of flow and sediment dynamics under separate and combined impacts of the illegal sand-mining, river encroachment, and upstream hydrological changes were simulated based on the calibrated model. The results obtained in this study could be useful to propose mitigation measures for riverbank erosion and accretion for management and monitoring

**Keywords:** Flow and sediment dynamics, hydrological alteration, MIKE 21, river encroachment, sand mining, Mekong River.

### INTRODUCTION

In recent years, riverbank erosion in the Vietnamese Mekong Delta (VMD) has been increased causing socio-economic losses. Thus, the riverbank erosion is considered as a complex natural disaster that is affected by human and natural factors. However, erosion problems are becoming exacerbated due to hydrological and sediment alteration as the result of upstream hydropower construction in combination with the sand mining, river encroachment, and waterway transportation activities. Hence, assessment of morphological changes should be taken account of scientists because of the complexity of the task. Furthermore, estimation of morphological dynamics plays an important role in controlling river systems and protecting human's livelihoods (Anthony et al., 2015).

Numerous approaches of assessing the morphological changes was implemented and applied including field measurement, morphological modeling, and remote sensing (Khoi et al., 2019). Among of them, the morphological modelling approach was widely used in scenario analysis, consisting MIKE 21, DELF3D, CCHE2D, and TELEMAC2D. Therefore, the MIKE 21 model was selected for this study because of its efficient

and powerful tool to assess the morphological changes under impacts of human and natural factors in Vietnam. In this study, we investigated the separate and combined impacts of human and natural factors on morphological change which is similar with other literature reviews.

The objective of this study is to investigate the response of flow and sediment dynamics under impacts of sand mining, river encroachment due to the expansion of fishponds, and hydrological alteration from the upstream area – a case study in the Mekong River in the Vinh Long province.

In order to achieve this objective, the main solution is to use the numerical models to simulate hydrodynamic and morphologic regimes of the Co Chien river, verified by the in-situ observation data. Therefore, using numerical mathematical models and combined measurement in some locations are necessary and effective in order to calibrate and validate obtained results from the model. The main aim of this study to provide comprehensive view of riverbed change in Co Chien River in a mega-delta from fluvial-dominated areas to tidal-dominated areas by using Mike 21. Hence, the obtained results from this study such as hydrodynamics, sediment transport and bed thickness

<sup>1</sup> Faculty of Civil Engineering, University of Technology, Vietnam National University Ho Chi Minh City, 268 Ly Thuong Kiet Street, District 10, Hochiminh City, VIETNAM

<sup>2</sup> Faculty of Environmental, University of Science, Vietnam National University Ho Chi Minh City, 227 Nguyen Van Cu Street, District 5, Hochiminh City, VIETNAM

<sup>3</sup> Faculty of Island Marine Resource Management, University of Natural Resources and Environment, 236B Le Van Sy Street, Tan Binh District, Hochiminh City, VIETNAM

change have a significant contribute to broaden horizontal knowledge in this topic.

**METHODOLOGY**

**Study area**

The study area is the segment of Co Chien River in Vung Liem district, Vinh Long province (river length about 15 km) and limited with three boundaries as in Fig. 1.

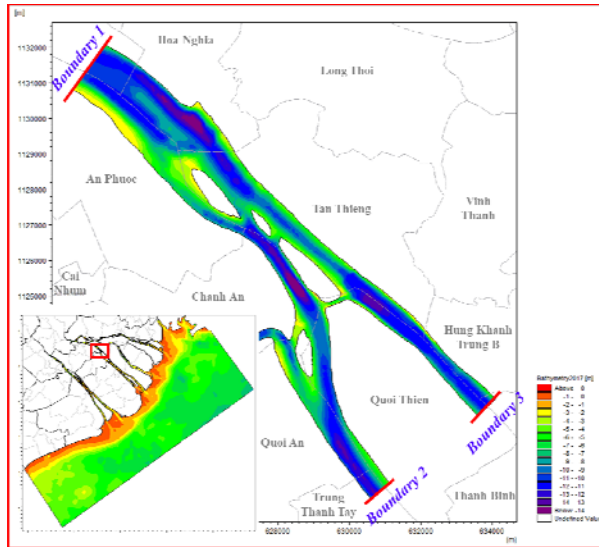


Fig. 1 Study area (Detailed model – Model 2)

The model used for this study area is the MIKE 21 FM with HD (hydrodynamic) and MT (mud transport) modules.

Model 1 (Regional model – Fig. 2) is a model for the entire the lower VMD (tidal-dominated zone) from My Thuan-Can Tho Bridge to the coastal area. The purpose of model 1 is to simulate flow regime and sediment transport regime to provide open boundaries for detailed model (model 2 – Fig. 1). The detailed model 2 was designed to assess hydrodynamic regime, sediment transport and morphological changes in the study area.

The bathymetry’s data in 2008 was provided by the Southern Institute of Water Resources Research.

Calculation mesh for model 2: unstructured mesh with 21145 elements, 11229 nodes, and the smallest angle of triangle elements is 26°, the distance between the nodes is 15 – 30m.

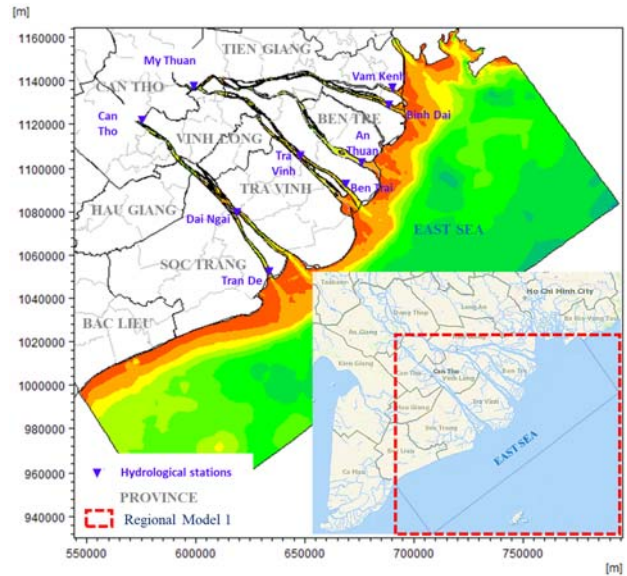


Fig. 2 Model for the entire the lower Vietnam Mekong Delta (VMD) (Regional model – Model 1)

**Basic theories**

**Hydraulic model Mike21 FM - HD module**

Integration of the horizontal momentum equations and the continuity equation over depth  $h = \eta + d$  the following two-dimensional (2D) shallow water equations are obtained:

Momentum equations:

$$\frac{\partial h\bar{u}}{\partial t} + \frac{\partial h\bar{u}^2}{\partial x} + \frac{\partial h\bar{v}\bar{u}}{\partial y} = f\bar{v}h - gh\frac{\partial\eta}{\partial x} - \frac{h}{\rho_0}\frac{\partial p_a}{\partial x} - \frac{gh^2}{2\rho_0}\frac{\partial\rho}{\partial x} + \frac{\tau_{sx}}{\rho_0} - \frac{\tau_{bx}}{\rho_0} - \frac{1}{\rho_0}\left(\frac{\partial s_{xx}}{\partial x} + \frac{\partial s_{xy}}{\partial y}\right) + \frac{\partial}{\partial x}(hT_{xx}) + \frac{\partial}{\partial y}(hT_{xy}) + hu_s S \tag{1}$$

$$\frac{\partial h\bar{v}}{\partial t} + \frac{\partial h\bar{v}^2}{\partial y} + \frac{\partial h\bar{v}\bar{u}}{\partial x} = f\bar{u}h - gh\frac{\partial\eta}{\partial y} - \frac{h}{\rho_0}\frac{\partial p_a}{\partial y} - \frac{gh^2}{2\rho_0}\frac{\partial\rho}{\partial y} + \frac{\tau_{sy}}{\rho_0} - \frac{\tau_{by}}{\rho_0} - \frac{1}{\rho_0}\left(\frac{\partial s_{yx}}{\partial x} + \frac{\partial s_{yy}}{\partial y}\right) + \frac{\partial}{\partial x}(hT_{xy}) + \frac{\partial}{\partial y}(hT_{yy}) + hv_s S \tag{2}$$

Continuous equation:

$$\frac{\partial h}{\partial t} + \frac{\partial h\bar{u}}{\partial x} + \frac{\partial h\bar{v}}{\partial y} = hS \tag{3}$$

where:

$h$ : Total water depth [m] ( $h = \eta + d$ )

$\eta$ : Water level [m]

$d$ : Still water depth [m]

$\bar{u}, \bar{v}$ : Depth – averaged horizontal velocity components in x, y direction [m/s]

$S$ : Magnitude of discharge [ $m^3/s/m^2$ ]

$\rho$ : Density of water [ $kg/m^3$ ]

$\tau_{sx}, \tau_{sy}$ : Surface wind stresses components in x, y direction [N/m<sup>2</sup>]

$\tau_{bx}, \tau_{by}$ : Bottom stresses components in x, y direction [N/m<sup>2</sup>]

f: Coriolis parameter

g: Gravitational acceleration [m/s<sup>2</sup>]

A: Horizontal eddy viscosity [m<sup>2</sup>/s]

S<sub>xx</sub>, S<sub>xy</sub>, S<sub>yy</sub>: Radiation stress tensor [N/m]

**Morphology model Mike21 FM - MT module**

The sediment transport formulations are based on the advection dispersion calculations in the Hydrodynamic module. The Mud Transport module solves the so-called advection-dispersion equation:

$$\frac{\partial \bar{c}}{\partial t} + u \frac{\partial \bar{c}}{\partial x} + v \frac{\partial \bar{c}}{\partial y} = \frac{1}{h} \frac{\partial}{\partial x} \left( h D_x \frac{\partial \bar{c}}{\partial x} \right) + \frac{1}{h} \frac{\partial}{\partial y} \left( h D_y \frac{\partial \bar{c}}{\partial y} \right) + Q_L C_L \frac{1}{h} + \frac{1}{h} \sum S \quad (4)$$

where:

$\bar{c}$ : Depth-average mass concentration [kg/m<sup>3</sup>]

u, v: Depth – averaged velocity [m/s]

D<sub>x</sub>, D<sub>y</sub>: Dispersion coefficients in x, y direction [m<sup>2</sup>/s]

h: Total water depth [m]

ΣS: Deposition/ erosion term [kg/m<sup>3</sup>/s]

Q<sub>L</sub>: Source discharge per unit horizontal area [m<sup>3</sup>/s/m<sup>2</sup>]

C<sub>L</sub>: Concentration of source discharge [kg/m<sup>3</sup>]

The thickness of the j<sup>th</sup> bed layer is a derived parameter determined as:

$$H_j^{new} = \frac{M_j}{\rho_{d,j}} = \frac{\sum_i m_{i,j}^{new}}{\rho_{d,j}} \quad (5)$$

H: Bed layer thickness [m]

M: Total sediment mass [kg/m<sup>2</sup>]

$\rho_d$ : Dry density [kg/m<sup>3</sup>]

**Model calibration/ validation**

The hydrodynamic and mud transport models were firstly calibrated with observation data of water level, discharge and total sediment suspended concentration (SSC) in April, 2012. Subsequently, the model was validated in October, 2017. Hydrological stations used for model calibration/ validation are presented in Fig. 2.

The model Mike 21HD with Manning number and viscosity coefficient may be used as calibration parameters in the modeling.

Due to the lack of detailed studies and measurements, the parameters describing the settling velocity, erosion, and deposition processes were estimated by the theory of Mike 21 MT model. By using the mean total SSC at My Thuan station, the corresponding settling velocities were

chosen as 0.003 m/s in the wet season. The critical shear stress for deposition was 0.01 N/m<sup>2</sup>, befitted the different sediment characteristics in the study area. In general, the critical shear stress for erosion is influenced by not only sediment characteristics but also by parameters of bed layers (Parchure et al., 1985; Partheniades, 1965). The values applied varied from 0.15 to 0.35 N/m<sup>2</sup> for the bottom layer. The erosion coefficient (E) is a proportion factor controlling by the erosion speed. It was set at 0.000002 kg/m<sup>2</sup>/s for the mud bed.

The model performance was assessed using statistical indices proposed by Moriasi et al. (2007), including: (1) Nash-Scutcliffe Efficiency (NSE) and Correlation coefficient (R<sup>2</sup>) used for assessing the model performance in the flow simulation, and (2) percent bias (PBias) used for assessing the model performance in the simulation of suspended sediment. The PBias index was used because the SSC data are quite sparse and discontinuous (SSC is measured twice per day (at the high and the low tide)) and PBIAS has the ability to clearly indicate poor model performance (Gupta et al., 1999).

The calibration and verification results of water level, water discharges and total SSC presented in Table 1 and Table 2.

Table 1 The discharge, water level results of calibration and validation at various positions in the study area

Stations		Calibration (1 – 30 April, 2012)		Validation (1 – 30 October, 2017)	
		NSE	R <sup>2</sup>	NSE	R <sup>2</sup>
Can Tho	Discharge	0.83	0.85	0.83	0.84
My Thuan		0.85	0.86	0.84	0.86
Can Tho	Water level	0.91	0.94	0.89	0.90
My Thuan		0.91	0.92	0.86	0.87
Tra Vinh		0.91	0.92	0.90	0.92
Vam Kenh		0.91	0.93	0.92	0.93
Binh Dai		0.94	0.94	0.92	0.93
An Thuan		0.93	0.93	0.92	0.93
Ben Trai		0.90	0.91	0.92	0.91
Tran De		0.91	0.92	0.92	0.92

Table 2 The total SSC results of calibration and validation at various positions in the study area

Stations	Calibration (01 – 30 April, 2012)	Validation (01 – 30 October, 2017)
	PBias	
Can Tho	14.1%	2.8%
My Thuan	3.5%	4.9%

There was an agreement between computed results and observation data in hydrodynamic (water level and discharge) and mud transport inform 2012 and 2017 and the result indicated that the hydrodynamic and mud transport models are well-calibrated.

**Modeling scenarios**

This report will assess the morphological changes under impacts of natural factors (SC0) and of human (reduction sediment flux – SC1, sand mining – SC2, extensions of fish ponds – SC3 and combined impacts of human – SC4).

In particular, the riverbank in 2008 was applied for three scenarios (SC0, SC1 and SC2); the riverbank in 2017 regarding the expansion of fishponds at Lac islet used in SC3 and SC4 (Fig. 3). Hydrological conditions were used following by 2008 and 2017 data (Table 3). Scenarios are summarized as shown in Table 4.

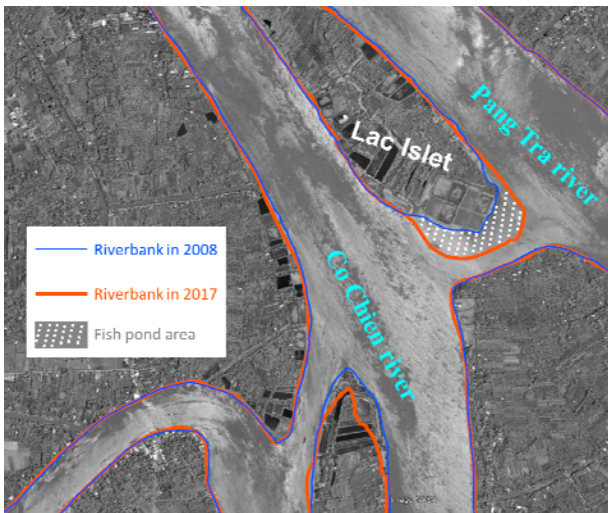


Fig. 3 Riverbank changes from 2008 to 2017

Table 3 Inflow into the Tien river

	2008	2017
Sediment flux (Mt/year)	59.82	38.84
Discharge (m <sup>3</sup> /s)	10730	11680

Table 4 The simulation scenarios

Scenarios	River bank	Hydrological conditions	Sand mining	Note
SC0		2008		Natural factors
SC1		2017		Reduction sediment inflow
SC2		2008	✓	Sand mining

SC3	2017	2008		Extension of fish ponds
SC4		2017	✓	Combined impacts of human

**RESULTS AND DISCUSSION**

The input hydrological data indicated that the inflow discharge of the Tien River in 2008 was less than 2017; however, the amount of sediment load in 2017 decreased by nearly 30% compared to 2008. Therefore, in the scenarios with hydrological conditions in 2008, the flow velocity was recognized as smaller, leading to more accretion than in 2017.

The computed results stated that analyzing current filed and total bed thickness change in the Co Chien River should be divided into two parts. The first part is around the Lac Islet, where river current interacts with two branch rivers. The second part is sand mining area in the Pang Tra river (Fig. 4).

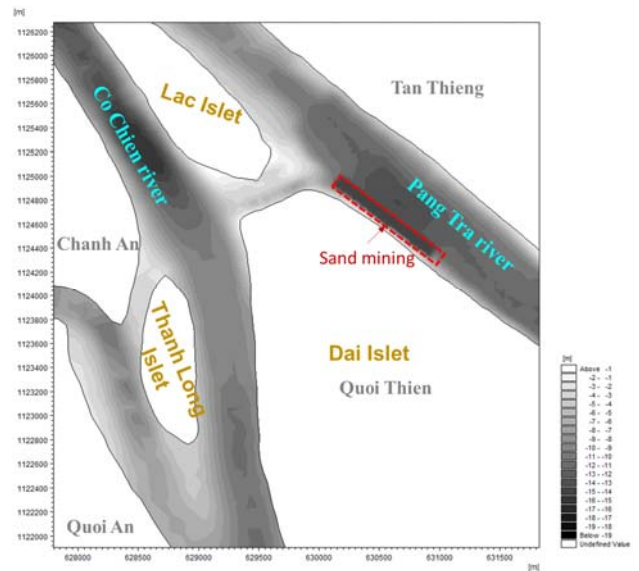


Fig. 4 Sand mining area

**SC0 – Natural scenario**

The velocity distribution of the Co Chien River was illustrated in Fig. 5. We found that high velocity values begin in the center of the river, moving closely to the riverbank. The maximum value of velocity in Co Chien River reached a peak at 1.37 m/s, whereas that value in midstream of Pang Tra River was 0.95 m/s. In addition to flow velocity in the Co Chien branch is larger than the Pang Tra branch in both directions, causing rapid accretion speed in the left branch.

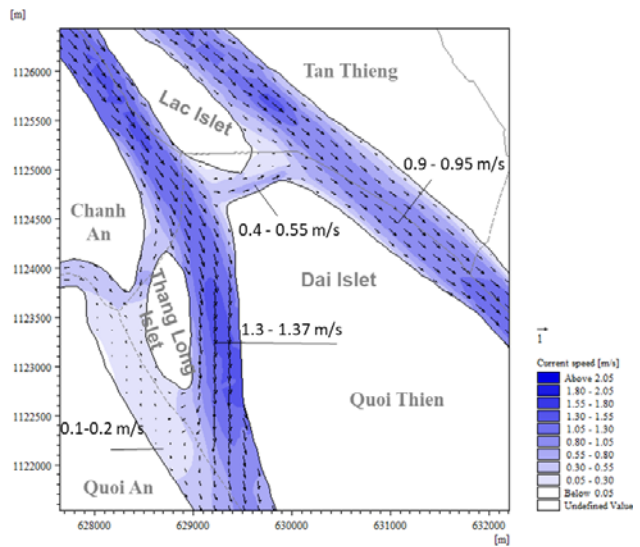
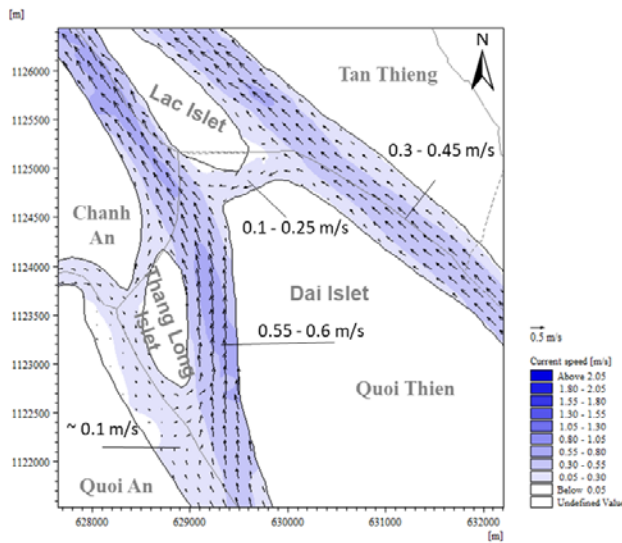


Fig. 5 Current speed of SC0

Total bed thickness change was presented below representative for deposition process with light to dark-blue color, erosion process with white color and white color was less erosion, and light to dark-red color stands for erosion after one-year simulation.

In general, segments of the river where the flow velocity changes suddenly were almost eroded (which has a strong flow velocity) (about > 0.7 m after one year – corresponding from white color to red color in the Fig. 6). The velocity at those locations was stronger because of the considerable riverbed depth. In addition, the weak cohesion of the geological structure is the main reason for erosion problems in this area, and it was good agreement with the observed data here.

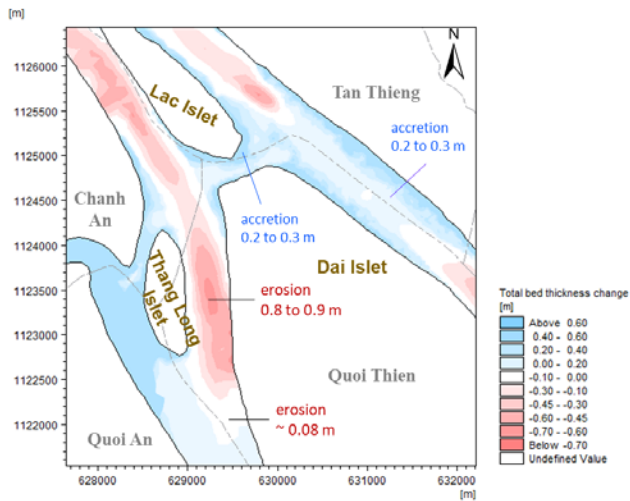


Fig. 6 Total bed thickness changes of SC0

**SC1 – Reduction sediment flux inflow**

In SC1, when the change of hydrological conditions regarding the 2017 data, the increase inflow discharge, the amount of sediment decreases and the current speed was higher than that of SC0 and the erosion problems occurs frequently (Fig. 7-8).

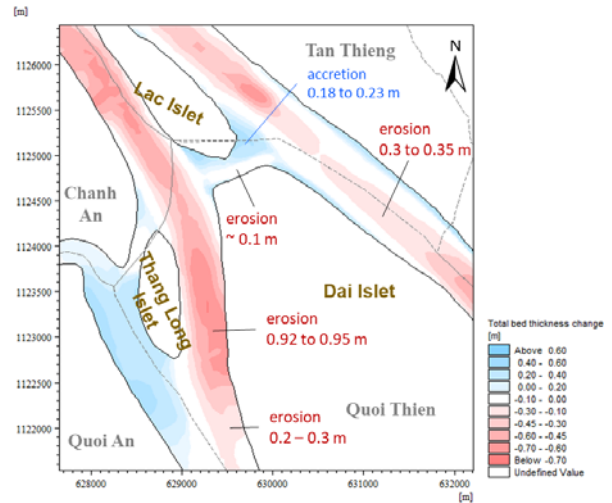


Fig. 7 Total bed thickness changes of SC1

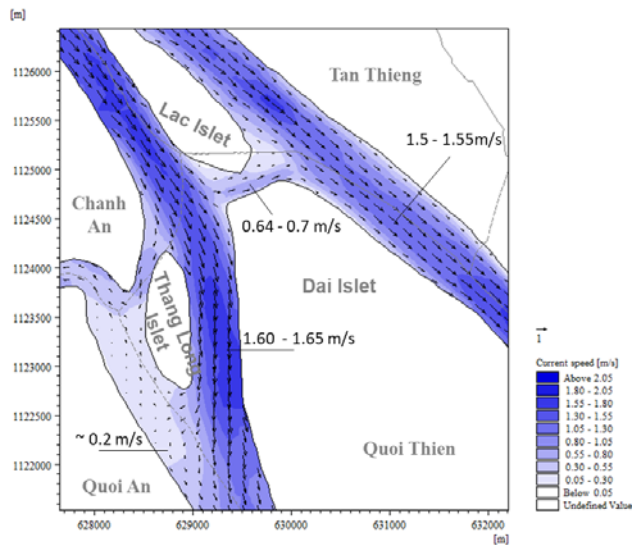
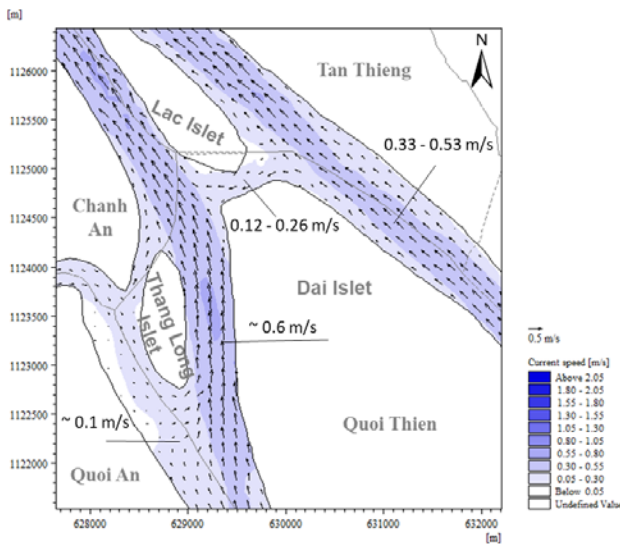


Fig. 8 Current speed of SC1

**SC2 – Sand mining**

It was very difficult to get the accurate statistic volume of the sand-mining, because, the limited observation data of sand mining activities. Furthermore, the reliable statistic of the sand-mining volume was insufficient, although the excessive sand-mining activity in the Co Chien River has been happen in a long period.

In SC2, sand-mining occurs at the same time, covering the entire lease areas with a constant dredging thickness with length 1000 m, width 100 m and depth 2 m (capacity approximately 200000 m<sup>3</sup>/year). The location of sand mining was selected in this report nearly to the right side Pang Tra river (Quoi Thien Commune) as shown in Fig. 4.

The SC2 results showed that with the same hydrological conditions as SC0, the flow velocity is unchanged. The sand-mining areas were not likely to capture sand and induce deficit in other areas resulting in erosion. The analysis results indicated that bottom erosion migration is limited to the immediate vicinity of the sand-mining area (Fig. 9). Due to siltation losses in the sand mining, the sediment imbalance leads to riverbed erosion. Therefore, management policy should be strictly to mitigate these problems.

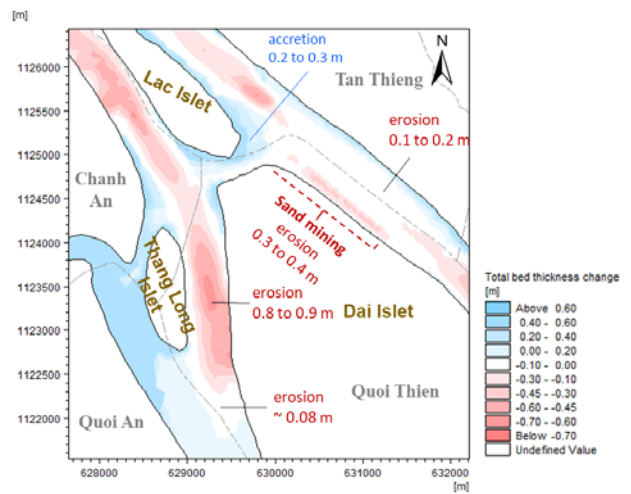


Fig. 9 Total bed thickness changes of SC2

**SC3 – Expansion of fishponds**

The river encroachment locations in the results of the expansion of the fish ponds were located in the riverside of Lac Islet with the riverbank in 2017 between Lac Islet and Dai Islet narrower riverbank in 2008. Since the flow was narrowed, the flow velocity was increased significantly, leading to bottom erosion in this area (Fig. 10 -11).

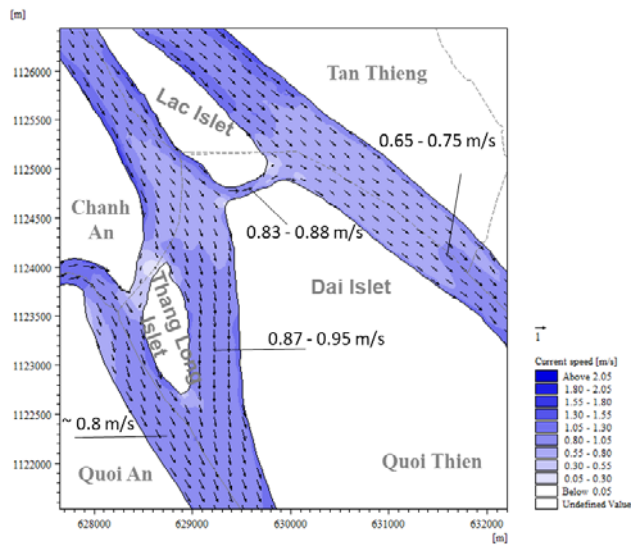
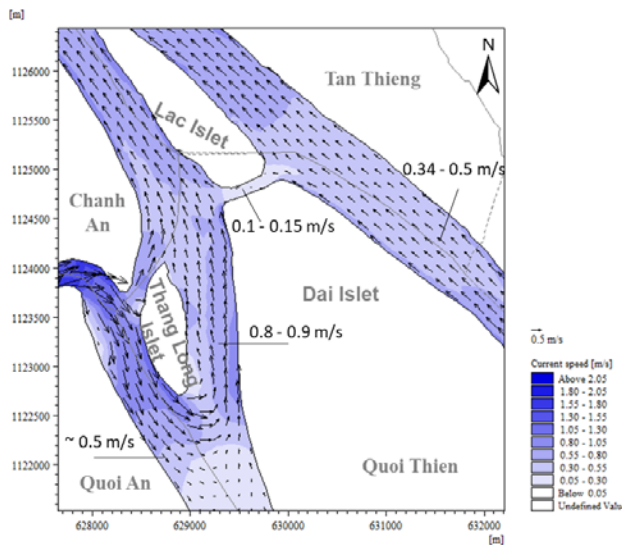


Fig. 10 Current speed of SC3

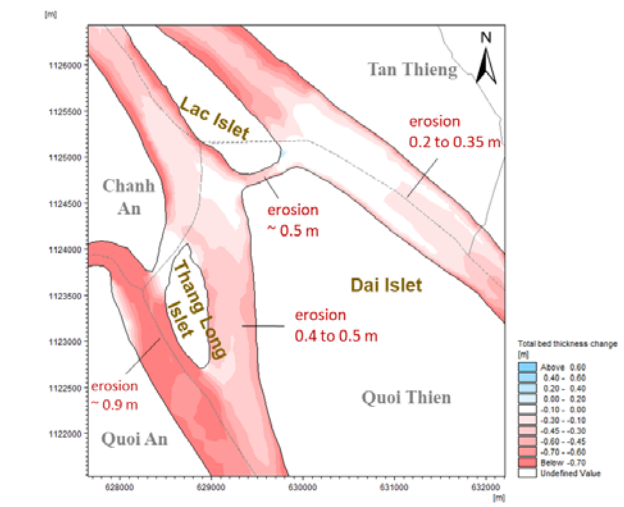
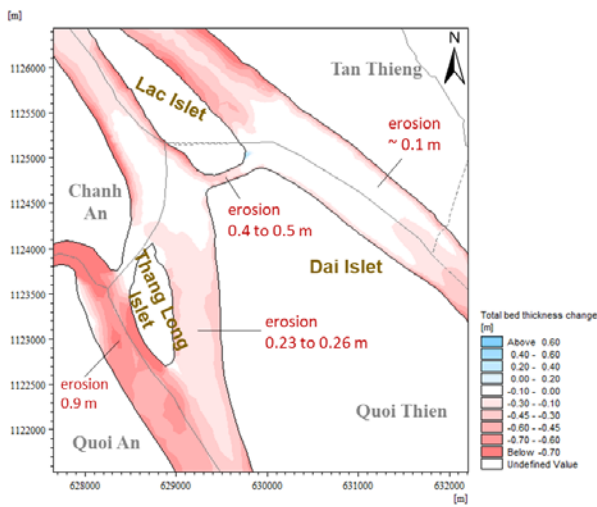


Fig. 12 Total bed thickness changes of SC4

**SC4 – Combined impact of human activities scenario**

Under the combined impacts of human activities scenario, riverbed changes have a negative tendency, causing to a rapid increase in erosion rates and a significant decrease in deposition rate (Fig. 12).

Table 5 summarized the Mike 21 results in five scenarios, and it showed that the current velocity in the Co Chien River was faster than that in the Pang Tra River. It is noticed that anthropogenic activities affect strongly on erosion problem in erosion-accretion processes.

Table 5 Simulation results

	Position	SC0	SC1	SC2	SC3	SC4
Current speed (m/s)	Co Chien River	0.5 – 1.37 m/s	0.6 – 1.65 m/s	0.55 – 1.39 m/s	0.8 – 0.95 m/s	0.57 – 1.8 m/s
	Pang Tra River	0.3 – 0.9 m/s	0.33 – 1.55 m/s	0.32 – 0.93 m/s	0.34 – 0.75 m/s	0.3 – 0.77 m/s
	Between Lac Islet and Dai Islet	0.1 -0.55 m/s	0.12 – 0.7 m/s	0.1 – 0.62 m/s	0.1 – 0.88 m/s	0.09 – 0.97 m/s

	Position	SC0	SC1	SC2	SC3	SC4
<b>Erosion/ Deposition rate (m/year)</b>	Co Chien River	Accretion 0.2 – 0.3 m (right branch Thang Long Islet) Erosion 0.3 – 0.4 m	Accretion ~ 0.2 m (right branch Thang Long Islet) Erosion 0.45 – 0.6 m	Accretion 0.2 – 0.3 m (right branch Thang Long Islet) Erosion 0.3 – 0.4 m	Erosion 0.23 – 0.9 m	Erosion 0.4 – 0.9 m
	Between Thang Long Islet and Dai Islet	Erosion 0.8 – 0.9 m (midstream to Dai Islet side)	Erosion 0.92 - 0.95 m (midstream to Dai Islet side)	Erosion 0.8 – 0.9 m (midstream to Dai Islet side)	Erosion 0.23– 0.26 m	Erosion 0.41 – 0.5 m
	Pang Tra River	Erosion 0.2 m Accretion 0.2 – 0.3 m (both riversides)	Erosion in midstream 0.3 – 0.45 m and ~0.1 m both riversides	Erosion 0.3 – 0.4 m (sand mining, near Dai Islet side) Accretion ~ 0.1 m (both riversides)	Erosion 0.1 - 0.5 m	Erosion 0.2 – 0.6 m (sand mining, near Dai Islet side)
	Between Lac Islet and Dai Islet	Accretion 0.2 – 0.3 m (both riverside)	Erosion ~0.1 m (Dai Islet side) Accretion 0.18-0.23 m (Lac Islet side)	Erosion ~0.1 m (Dai Islet side) Accretion 0.18-0.3 m (Lac Islet side)	Erosion 0.4 - 0.5 m (both riverside)	Erosion ~ 0.5 m (both riverside)

## CONCLUSION

The two-dimensional model simulating the hydrodynamic regimes under the combined influence of natural, sand mining and river encroachment scenarios has been developed. Considering the goodness-of-fit and reliable statistics of verification and simulation results, it is concluded that the model is suitable for simulate the discharge, sediment transport and erosion-accretion processes for Co Chien River in Vung Liem District (Vinh Long province).

The results showed that the current speed in the Co Chien River was stronger than that in the Pang Tra River in all conditions.

The sand-mining areas induced sediment deficit in vicinity areas, imbalance of mud and sand resulting in erosion (SC2).

When the flow was narrowed by the expansion of the fish ponds (SC3 and SC4), the flow velocity was increased significantly, leading to bottom erosion.

In conclusion, anthropogenic activities affect strongly on morphology changes. Therefore, management policy should be strictly to mitigate these problems.

## ACKNOWLEDGEMENTS

This research is funded by Ministry of Science and Technology of Vietnam under the grant number “KH-CN-TNB.ĐT /14-19/C10”.

## REFERENCES

Anthony, E.J., Brunier, G., Besset, M., Goichot, M., Dussouillez, P., Nguyen, V.L. (2015). Linking rapid erosion of the Mekong River delta to human activities. *Sci. Rep.* 5, 14745.

Gupta, H. V., S. Sorooshian, and P. O. Yapo. 1999. Status of automatic calibration for hydrologic models: Comparison with multilevel expert calibration. *J. Hydrologic Eng.* 4(2): 135-143.

Khoi, D.N., Dang, T.D., Pham, L.T.H., Phung, N.K., and Bay, N.T. (2019). Morphological change assessment from intertidal to river-dominated zones using multiple-satellite imagery – a case study of the Vietnamese Mekong Delta. *Regional Studies in Marine Science.* (Accepted).

Letrung, T., Ngoc, T.A., Hiramatsu, K. (2016). Effect of the Interaction Between Monsoon Currents and Waves on the Morphological Processes along the Mekong River Delta Coast. *Japan Agric. Res. Q. JARQ* 50, 121–133.

Li, X., Liu, J.P., Saito, Y., Nguyen, V.L. (2017). Recent evolution of the Mekong Delta and the impacts of dams. *Earth-Science Rev.* 175, 1–17.

Liu, P., DeMaster, D., Nguyen, T., Saito, Y., Nguyen, V.L., Ta, T.K.O., Li, X., (2017). Stratigraphic Formation of the Mekong River Delta and Its Recent Shoreline Changes. *Oceanography* 30, 72–83.

Moriasi, D.N., Arnold, J. G., Van Liew, M. W., Bingner, R. L., Harmel, R. D., Veith, T. L., (2007). Model evaluation guidelines for systematic quantification of accuracy in watershed simulations. *Trans. ASABE* 50:3, 885-900.

Parchure, T.M., Mehta, A.J., (1985). Erosion of soft cohesive sediment deposits. *J. Hydraulic Engineering, ASCE* 111 (10), 1308–1326.

Partheniades, E. (1965). Erosion and deposition of cohesive soils. *J. Hydraul. Div. Proc., ASCE* 91 (HY1), 105–139.